Int. J. Multiphase Flow, Vol. 2, pp. 495–520. Pergamon/Elsevier, 1976. Printed in Great Britain.

INTERPRETATION OF INTERNAL TRACER EXPERIMENTS AND LOCAL SOJOURN TIME DISTRIBUTIONS

Y. ZVIRIN† and R. SHINNAR

Department of Chemical Engineering, The City College of the City University of New York, NY 10031, U.S.A.

(*Received* 20 *January* 1974)

Abstract—Tracer experiments are a valuable tool in the study of transport phenomena. Most of the theoretical work about tracers has been concerned either with systems having clearly defined inlet and outlet or with recirculating flows. In this article the methods are generalized to more complex situations and an attempt is made to provide a uniform theoretical treatment for local tracer experiments performed at several sites inside the flow systems. Local purging rate and mixing rate are defined and their measurements and applications are discussed. Several sojourn time distributions are discussed, especially that of local remaining life which might be useful in the study of local processes in large flow systems. The results should be of interest in a wide variety of areas in which tracer experiments are used, such as chemical reactor design, physiology, hydrology and the study of dispersion processes in the atmosphere and in oceans.

1. INTRODUCTION

The use of tracers for investigating flow systems, especially in the fields of water physiology and coastal pollution, has become more and more frequent in recent years. The appearance of new tracers and the development of more sensitive methods of detection imply even more extensive use in the future. Tracer methods are used for various purposes: determination of the physical parameters of systems, e.g. flow rates (Clayton & Smith 1963; Dinger 1967); diffusion, dispersion and dilution coefficients (Selleck & Pearson 1961; Harleman *et al.* 1966; Harremoes 1966; Barrett *et al.* 1969; Okubo & Pritchard 1969); reaeration coefficients (Tsivoglou *et al.* 1968); justification of analytical methods (O'Connor 1962, 1966); modelling of flow systems (Ingram *et al.* 1966); and tracing of sand transport in coastal waters (Duane 1970).

Most of the theoretical framework developed for tracer experiments in the different disciplines have dealt with some special types of open systems, which have one clearly defined inlet and outlet (Zierler 1962; Aris 1966). Some aspects of the theory of tracers for more general systems were investigated by Hart (1960) and Bergner (1961). Naor, Shinnar & Katz (1963, 1967, 1972a,b), outlined the method of regarding the behavior of tracers as stochastic processes and also demonstrated the equivalence of diffusional and compartmental models.

The main use of tracer experiments in flow systems is to evaluate some parameters of a model representing the system. Therefore, the results are usually strongly dependent on the model chosen. For example, Obrist *et al.* (1967) reported a considerable difference between the descriptions of cerebral blood flow by two and three-compartment models. Moreover, several tracer experiments can yield global model-free parameters of flow systems. Consider, for example, a system with a single inlet and a single outlet. It is well known that by an experiment of inserting tracer in the inlet and measurement of the resulting concentration at the outlet, the flow rate can be determined quite accurately. In principle, the volume of the system can be calculated from the first moment of the concentration vs time curve. However, the error involved in this calculation can be rather large, and furthermore, the volume computed from this experiment is of the active (flushed) part of the system, while stagnant regions can hardly be detected. Local properties of the system can be determined by the existing tracer methods only on the basis of diffusional or compartmental models. The errors in the evaluation of local parameters are mostly larger, e.g. when the diffusion coefficient in a one-dimensional single inlet–single outlet system is determined by the second moment of the concentration vs time curve.

†*Present address*: Faculty of Mechanical Engineering, Technion—Israel Institute of Technology, Haifa, Israel.

In systems with multiple inlets and outlets the problem is even more difficult. There does not exist any definition of a local flow rate which would describe the local flow situation. Velocity profiles can answer the problem but these are usually hard (or expensive) to obtain.

The purpose of the present work is to develop a more general approach for the interpretation of tracer experiments in the study of transport processes in flow systems with multiple inlets and outlets. A method for the description of these processes is suggested, based on the definition of local model free parameters—the purging rate (section 3), the mixing rate and the equivalent Peclet number (section 4) and local sojourn time distributions such as the remaining life distribution (section 5). These parameters can be determined directly from tracer measurements, without resorting to any model. Their values and especially their spatial distributions in the system describe the nature of the mixing and purging (or flushing) processes in the system.

We discuss experiments in which tracer is introduced at some points within the system and the resulting concentration histories are measured at the same points and other sites. It is assumed that the system is steady, or if there are turbulent transport processes, the average local tracer responses are steady.

Compartmental analysis is used for the definition of the above-mentioned model free parameters. However, this is not a limitation and we do not assume that the system really consists of stirred tanks. The model free parameters defined in this work are general and not restricted to any system or any model which represents it. These parameters are directly determined by the tracer measurements. Indeed, Shinnar & Naor (1967) showed that the continuous (diffusional) behavior can be obtained from the compartmental model when the number of compartments tends to infinity. In section 6, an example of a two-phase flow is treated by both models and their equivalence is shown on the basis of the model free parameters.

2. GENERAL TRACER EXPERIMENTS

The behavior of a general flow system is described here on the basis of compartmental analysis and probability theory. The system can be represented by the set of transition probabilities, which are directly related to the concentration histories of tracer material introduced into the system. It is assumed that the system is in steady state and the compartments have constant volumes. Generalizations to other situations are available to some part (Hart 1960).

Consider a network consisting of n compartments (or vessels), having volumes V_i. W_{ij} is the flow rate from vessel i to j, W_i^e and W_i^f are the outflow and inflow rates for vessel i, respectively. Denote:

$$W_{ii} = -\sum_{j \neq i} W_{ij} - W_i^e \qquad i, j = 1, 2, \ldots, n. \tag{1}$$

Then by definition:

$$\sum_j W_{ij} = -W_i^e, \tag{2}$$

and by material balance:

$$\sum_i W_{ij} = -W_j^f. \tag{3}$$

Denote, further, the modified flow rates by:

$$w_{ij} \equiv W_{ij}/V_i; \quad w_i^e \equiv W_i^e/V_i; \quad w_i^f \equiv W_i^f/V_i. \tag{4}$$

Denote the transition probability from vessel i to j by $p_{ij}(t)$ and from i to the outlet of j by $p_{ij}^e(t)$ where t is the time.

The transition probabilities are directly related to the concentrations of the tracer material in the various vessels: inject an amount m of tracer in vessel i as a pulse at $t = 0$ and measure the concentration of the tracer material $c_j(t)$ at vessel j. The transition probability is simply the ratio of the amounts of tracer material:

$$p_{ij}(t) = \frac{c_j(t) V_j}{m}. \qquad [5]$$

It is noted that the same results can be obtained from the step experiment, in which tracer is injected at a constant rate.

We further assume that for single molecules the processes can be considered as Markovian; this is no real limitation on the applicability of the results as explained by Bergner (1961) and Krambeck *et al.* (1969*a*, *b*). Thus the governing equations for transition probabilities are either the "backward" equations:

$$\frac{dp_{ij}}{dt} = \sum_k w_{ik} p_{kj} \qquad i, j, k = 1, 2, \ldots, n \qquad [6]$$

$$\frac{dp^e_{ij}}{dt} = \sum_k w_{ik} p^e_{kj} + w_i^e \delta_{ij} \qquad [7]$$

which are obtained by material balance of vessel i, or the "forward" equations:

$$\frac{dp_{ij}}{dt} = \sum_k p_{ik} w_{kj} \qquad [8]$$

$$\frac{dp^e_{ij}}{dt} = p_{ij} w_j^e \qquad [9]$$

which can be obtained by material balance of vessel j. The initial conditions are:

$$p^{(0)}_{ij} = \delta_{ij} \qquad i, j = 1, 2, \ldots, n \qquad [10]$$

$$p^e_{ij}(0) = 0 \qquad [11]$$

where δ_{ij} is the Kroenecker δ.

Several relationships can be derived from the equations before solving them. In particular, we are interested in the following one:

$$\sum_i W_i^f \int_0^\infty p_{ij}(t)\, dt = V_j \qquad [12]$$

which is obtained from [3], [5] and [6]. This relationship will be used in the next section for the definition of the purging rate.

The solution for [6] or [8] with the initial conditions [10] is given by:

$$p_{ij}(t) = \sum_k A^k_{ij} e^{\lambda_k t} \qquad i, j, k = 1, 2, \ldots, n \qquad [13]$$

where λ_k are the eigenvalues of the matrix $\mathbf{w} = (w_{ij})$ and the coefficients A^k_{ij} are given by:

$$A^k_{ij} = S_i^k R_j^k \qquad [14]$$

where $\mathbf{S}^k$ and $\mathbf{R}^k$ are the row and column eigenvectors of $\mathbf{w}$, given by:

$$\mathbf{w} \cdot \mathbf{S}^k = \lambda_k \mathbf{S}^k; \quad \mathbf{R}^k \cdot \mathbf{w} = \lambda_k \mathbf{R}^k. \tag{15}$$

The eigenvalues λ_k may be complex, but it has been established by Hearon (1963) that for all physically realizable cases, when the flow rates w_{ij} $(i \neq j)$ are non-negative, λ_k have negative real parts. When there are repeated values of the eigenvalues, the solution [13] has to be modified, cf. Hearon (1963).

The transition probabilities p_{ij} can be determined by tracer experiments of injecting the tracer in vessel i and measuring the concentration history at vessel j. Obviously, all the elements of the matrix $\mathbf{p}$ of the transition probabilities can be determined by n^2 measurements, and then all the elements of the matrix $\mathbf{w}$ can be calculated, cf. Hart (1963). In principle, however, as shown in Appendix A, only n measurements are necessary to determine all the flow rates of the network, if the geometry (the volumes) of the system is known.

As mentioned above, tracer experiments are often used for the evaluation of model parameters. The identification of the eigenvalues λ_k can be done, for example, by "peeling" the exponentials [13] of measured concentration curves, starting from the tail which is dominated by the first (smallest absolute value) eigenvalue, cf. Obrist *et al.* (1967). This method is generally inaccurate because it relies on the tail, where the concentration is small and hard to detect and also because the experiment is truncated after a finite time. Moreover, it will fail when the number of vessels is large and especially when the eigenvalues are complex numbers as in cases of recirculation.

Another method is the direct estimation of the flow rates from the concentration measurements, using [6] or [8]. Values of the transition probabilities from [5] and their time derivatives are introduced into these equations, yielding a set of linear algebraic equations for the flow rates. The number of equations must not be smaller than the number of unknown flow rates. However, a large number of equations, i.e. from several times, can be set and the solution then can be made using variational methods, such as that of the least squares, cf. Graupe (1972).

As mentioned above, the compartmental analysis is not used in this work for the identification of model parameters. It is used in the following sections for the definitions of the model free parameters—purging rate, equivalent Peclet number and several sojourn time distributions.

3. THE LOCAL PURGING RATE

The local flow conditions in a system can be described on the basis of a compartmental model. In order to determine the model parameters by tracer experiments, measurements (or injections) of the tracer are required in all regions of the system, as shown in the previous section. The same is also true for diffusional models representing non-uniform systems. One is then tempted to search for some simpler local flow properties that can be both defined and measured on a local scale. A parameter suitable for this purpose is the local purging rate, defined below.

Let us start with a system having a single inlet. The inflow rate W^f can be directly determined by introducing tracer in the inlet and measuring the concentration at any point within the system:

$$W^f = \begin{cases} \dfrac{q}{c_j(\infty)} & \text{step experiment} \\ \dfrac{m}{\int_0^\infty c_i(t)\,\mathrm{d}t} & \text{pulse experiment} \end{cases} \tag{16}$$

where m is the amount of tracer injected in a pulse experiment and q is the rate of tracer input in a step experiment.

We note that the flow rate measured by this type of experiment refers to the inflow only and not to any internal local properties, not even at the measuring point. The same is true if there is a

single outlet and several inlets. We can inject the tracer then at any point in the system; if we measure the concentration $c_e(t)$ at the outlet, [16] gives the correct outflow rate. The accuracy of the measurement depends (and often very significantly) on the injection (or measuring) point. Thus, measuring (or injecting) in a stagnant region yields the same value of $c(\infty)$ for a step experiment, but the time needed to reach $c(\infty)$ is longer. Here, however, we are looking for a flow rate which is a local property and will enable us to distinguish between well purged and stagnant regions. Consider a pulse or a step experiment, in which tracer is introduced into vessel j and the resulting concentration history in this vessel $c_j(t)$ is measured. We define the purging rate U_j at vessel j by:

$$U_j = \begin{cases} \dfrac{m}{\int_0^\infty c_j \, dt} & \text{pulse} \\ \dfrac{q}{c_j(\infty)} & \text{step} \end{cases} \qquad j = 1, 2, \ldots, n. \tag{17}$$

As will be shown later, the purging rate U_j represents the total net rate at which particles present at vessel j are transported towards the outlets. The generalization to a continuous system is obvious: the purging rate is given by [17] where j simply denotes any point within the system.

Let us now show that the purging rate defined by [17] is a true local property, which is model-free and is independent of the details of the tracer experiment.

For a pulse experiment, it follows from [17] and [5] that:

$$U_j = V_j / \int_0^\infty p_{jj}(t) \, dt. \tag{18}$$

It is shown in appendix B that the probability P_{ij} of a particle at i to pass through j is given by:

$$P_{ij} = \int_0^\infty p_{ij}(t) \, dt \Big/ \int_0^\infty P_{ij}(t) \, dt \, . \tag{19}$$

Introducing [19] into [12] and using [18], the following relation is obtained for the purging rate:

$$U_j = \sum_k W_k^f p_{kj}. \tag{20}$$

Thus U_j is the fraction of the total flow through the system which passes at vessel j on its way to the outlets. In a similar way, it can be shown that:

$$U_j = \sum_i Q_{ji} W_i^e \tag{21}$$

where Q_{ji} is the probability that a particle at i has passed (at least once) through j.

Finally, from [18], [19] and [12] the following expression for the purging rate is obtained:

$$U_j = \frac{m}{\int_0^\infty c_{ij}(t) \, dt} P_{ij}. \tag{22}$$

The last form can be employed to measure the purging rate from an i to j tracer experiment, when P_{ij} is known. This can be useful for a system with a single outlet, where the measuring point j is on the way to the outlet and $P_{ij} = 1$.

The purging rate depends on both convection and diffusion in a local region, and it also includes information about the connection of the region to the other parts of the system. Thus, for example, the purging rate is small for a region with strong local mixing, which is weakly connected to the other regions. Such a region is stagnant, and this can easily be detected by an appropriate tracer experiment, and measurement of the purging rate by [17] or [19]. Theoretically, the same information can be obtained from an inlet-to-outlet experiment; however, in that case the information is contained in the tail of the concentration curve. Moreover, since the measurement is truncated at a finite time, any information based on the tail is inaccurate in most cases.

Another significance of the purging rate can be observed from [18]. Consider the probability density $\pi_{ij}(t)$ that a particle is in vessel j at the time interval between t and $t+\mathrm{d}t$:

$$\pi_{ii} = \frac{p_{ji}(t)}{\int_0^\infty p_{ij}(t)\,\mathrm{d}t}. \qquad [23]$$

U_i is related to $\pi_{ji}(t)$ just as the inflow rate W^f relates the average residence time distribution $\bar{t}$ and the volume V of a single inlet–single outlet system:

$$W^f = W^e = W = \frac{V}{\bar{t}}. \qquad [24]$$

This property of the purging rate is discussed further in section 5.

As an application for the use of the purging rate [17], consider the well known method of checking the functioning of the liver. A solution of indocyanine green is injected at a constant rate into an artery and the resulting steady state concentration is measured at the same site, c.f. Bassingthwaighte (1974). The measurement gives the local purging rate i.e. the rate at which the indocyanine green is transported from the site of injection to the liver and excreted there. Actually this test is not intended to measure the local property (at the artery), but the excretion through the

Table 1. Printout of peak counts/sec and time

59	58	197	83	158	118	205	189	152	181	183	137
179	147	172	142	178	176	178	149	150	173	5	172
54	79	156	81	166	105	123	219	114	182	213	132
131	162	149	125	122	134	130	5	5	5	6	5
99	82	167	80	126	155	396	488	327	261	274	106
169	162	165	149	152	117	5	5	5	5	5	107
83	111	150	100	242	399	461	661	615	447	229	108
171	179	121	140	7	5	5	5	5	5	5	94
133	124	149	125	515	461	496	374	355	294	189	116
151	144	150	114	7	7	7	5	5	5	5	95
158	113	172	241	623	447	358	377	173	148	160	117
157	139	128	7	7	7	10	7	7	113	111	89
124	138	292	416	742	325	409	371	112	151	130	109
118	126	14	8	7	7	7	8	64	77	111	72
157	134	442	457	678	318	622	310	113	151	147	146
117	152	13	9	7	8	8	11	68	107	65	81
110	147	329	298	422	272	295	181	113	150	150	108
107	81	9	8	8	8	9	71	108	76	82	85
137	130	401	376	458	249	331	212	132	181	155	123
75	110	9	8	8	9	10	88	71	67	86	63
114	106	304	296	394	218	212	215	127	120	121	100
125	117	9	8	16	11	60	85	56	78	81	68
109	89	117	140	108	117	179	190	107	109	104	106
125	141	154	70	109	88	69	65	66	65	60	94

A portion of the computer output depicting the peak counts/sec recorded by each crystal (top number) and the number of seconds after the start of the study when peak counts/sec occurred in each crystal is presented. The peak counts/sec were higher and occurred sooner in crystals overlying myocardium than in those overlying the lungs. From Cannon *et al.* (1972).

liver. The reason that these two are almost equivalent is due to the fact that the mixing in the large circulation is much faster than the rate of excretion. A different result would be obtained from an injection in a stagnant vein. The local purging rate in that case will reflect the local transport phenomenon and not the operation of the liver.

Another way of measuring the purging rate, according to [20] can be applied to the results of Cannon *et al.* (1972). They investigated regional myocardial perfusion rates in humans, using injection of ^{133}Xe at the inlet and measuring the resulting regional activities by a scintillation camera. The area beneath any activity versus time curve would give the same value, which is proportional to the inflow rate and is not a local property. Cannon *et al.* noticed that the peak counts per minute occured rather quickly and after approximately the same time for the whole myocardium (see table 1). This suggests that the system can be considered as consisting of many

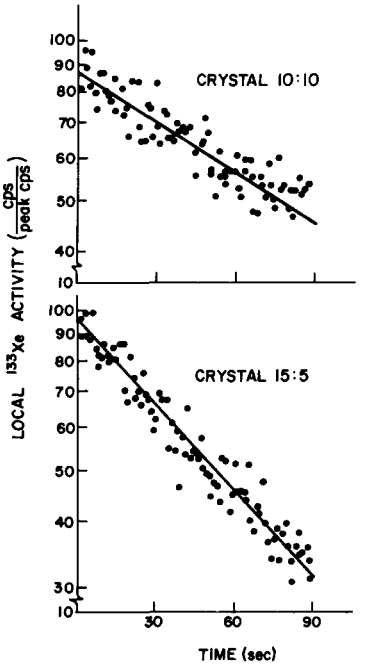

Figure 1. Two semilogarithmic plots of myocardial ^{133}Xe activity (cps/peak cps against time) are depicted. These were obtained by two crystals in one patient. The patient had coronary artery disease; one crystal overlay myocardium supplied by a normal vessel (bottom); The other (top) was over tissue supplied by a narrowed branch of the left coronary. From Cannon *et al.* (1972).

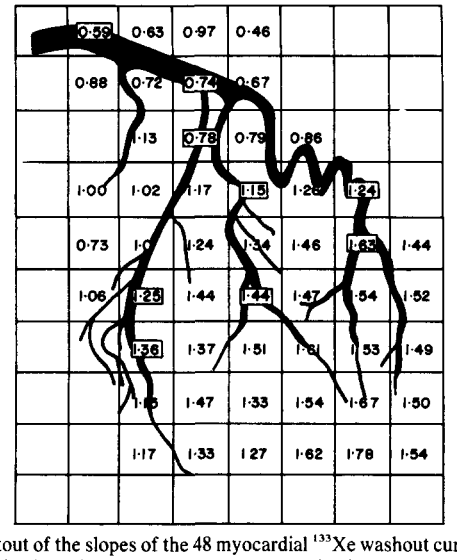

Figure 2. A computer printout of the slopes of the 48 myocardial ^{133}Xe washout curves obtained after a single left coronary injection in patient H. W. is shown (A–P projection). From Cannon *et al.* (1972).

compartments connected separately to a main stream of strong plug flow. Cannon *et al.* Computed regional perfusion rates from the slopes of single exponential decay curves, fitted to the experimental measurements (by a least squares procedure), see figures 1 and 2. This method is similar to the washout curve measurement.

The same results can be obtained directly by measuring the areas beneath the concentration curves normalized by the peak concentration. These will immediately give the local purging rates and thus the numerical procedure of fitting the curves becomes unnecessary. The spatial variation of the purging rate indicates the functioning of the various regions, as explained above.

4. THE LOCAL MIXING RATE AND THE EQUIVALENT PECLET NUMBER

Another desired local parameter would be the local mixing rate, or the rate at which vessel j interchanges fluids with its surroundings. For a given network of stirred tanks the obvious definition of this rate is the turnover rate suggested by Bergner (1961)

$$T_i = -W_{ii} = \sum_{j \neq i} W_{ij} + W_i^e. \qquad [25]$$

There are two disadvantages in choosing this definition. First, T_i is not directly measurable. In order to determine it, measurements at i and several neighboring regions are needed and T_i is then calculated on the basis of some model, at least for the vicinity of i. Moreover, the turnover rate increases and tends to infinity when the number of vessels is increased to approach the description of the continuous systems.

The latter difficulty can be avoided by defining an equivalent Peclet number which will tend to a finite value for continuous systems. However, the equivalent Peclet number also cannot be measured directly.

When modelling a complex flow, the network that represents it is not unique. For high accuracy we would need a very large number of vessels, but for practical purposes we can have good approximations with quite a small number. Consider the case where the flow is one dimensional with a net flow rate W, a diffusion coefficient D and a constant cross-section A. The system can be described by the diffusion equation:

$$\frac{\partial c}{\partial t} + \frac{W}{A}\frac{\partial c}{\partial x} - D\frac{\partial^2 c}{\partial x^2} = 0 \qquad [26]$$

with boundary and initial conditions:

$$\frac{W}{A}c - D\frac{\partial c}{\partial x} = 0 \qquad \text{at } x = 0, \qquad [27a]$$

$$\frac{\partial c}{\partial x} = 0 \qquad \text{at } x = L, \qquad [27b]$$

$$c = 0 \qquad \text{at } t = 0. \qquad [27c]$$

This flow can be approximated for all practical purposes by a cascade of stirred tanks (figure 3) with forward and backward flows as long as the number of stirred tanks is larger than half the Peclet number WL/DA. Even if we take a cascade of $n = WL/2DA$ stirred tanks with forward flows only the approximation will be sufficient for most purposes. For $n = WL/2DA$ the turnover rate will be W^f, but as n increases the turnover rate approaches infinity. What we are looking for is a local Peclet number related to the turnover rate in such a way that models with similar overall properties will have local Peclet numbers which are not sensitive to the number of tanks used.

For the cascade shown in figure 3, it will be shown that the following expression:

$$\rho_i = \frac{2V}{V_i}\frac{W}{T_i} = \frac{1-\pi}{1+\pi}2n \qquad [28]$$

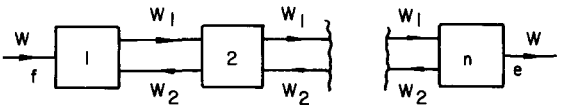

Figure 3. A cascade of stirred tanks representing a one-dimensional flow with back-mixing.

where V is the total volume of the system and

$$\pi = W_2/(W_2 + W),$$

fulfills these conditions very well. Equation [28] defines as an equivalent Peclet number the ratio of the net flow rate (equal in this case to the purging rate) to the turnover rate normalized by the ratio of the local volume to the total volume. The factor 2 will be explained later. As $n \to \infty$ the above model will approach correctly the flow described by [26]–[27] as was shown by Naor & Shinnar (1967). While T_i will approach infinity, $T_i V_i$ remains finite. There are obviously many other ways in which we could define such a Peclet number. Thus, Naor & Shinnar (1967) used the following definitions

$$\rho' = n(1 - \pi). \qquad [29]$$

For large n there is very little difference between the two (as $1 + \pi = 2$). For small n it is found that the group defined in [28] has some remarkable advantages. As an example, consider the coefficient of variation γ^2 of the residence time distribution given by Naor & Shinnar (1967):

$$\gamma^2 = \frac{\sigma^2}{\bar{t}^2} = \frac{1}{n} + \frac{2\pi}{[n(1-\pi)]^2}(n-1) - n\pi + \pi^2, \qquad [30]$$

where σ^2 is the variance and $\bar{t}$ is the average of the distribution (see also section 5 here). In figure 4, γ^2 is plotted vs the equivalent Peclet number defined by [29], and in figure 5, as defined by [28]. It is noted that for the latter, the variance changes very little over the whole range. Obviously the larger n the better the overall fit between the system described by [26]–[27] and the compartmental model. But even a rather small n (the smallest n is $WL/2DA$), gives a very good description, and is sufficient for many purposes.

This desire for a good fit for small n now implies why the factor 2 was introduced in the definition [28] for ρ_i.

The Peclet number defined by [28] has another interesting property. Consider for example a cascade of five stirred tanks in series with forward flow only, where $\pi = 0$ and the Peclet number

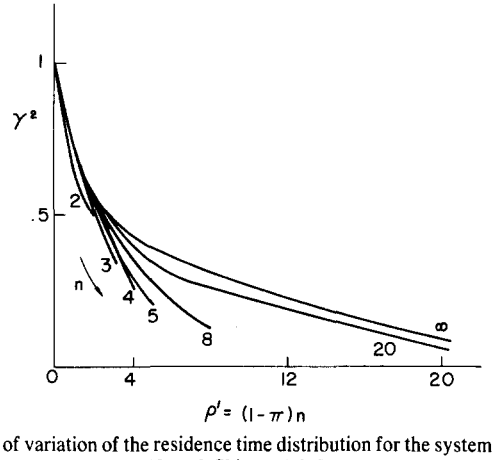

Figure 4. The coefficient of variation of the residence time distribution for the system shown in figure 3. From Naor & Shinnar (1967).

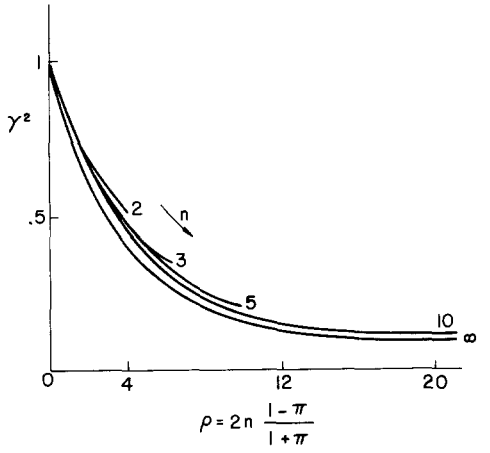

Figure 5. The coefficient of variation of the residence time distribution for the system shown in figure 3. The Peclet number is defined as in [28].

ρ is 10. There is no backflow and, therefore, no flows related to mixing between the vessels. However, the fact that a cascade of five vessels can describe the system already indicates a local backmixing phenomena represented by the Peclet number.

Expression [28] was derived for a rather simple case. For more general three-dimensional systems we can generalize it by substituting the purging rate for W. Thus, the Peclet number in vessel i is defined by:

$$\rho_i = \frac{2V}{V_i}\frac{U_i}{T_i}. \qquad [31]$$

ρ_i is a local property and its spatial distribution in the system gives also an indication about the uniformity of the mixing processes.

The equivalent Peclet number as defined by [31] depends on the model chosen to represent the system (or on the compartmentalization). Unlike the purging rate, the turnover rate T_i cannot be measured directly. It can be obtained only by several measurements and calculations on the basis of some model for the system or at least for the region in question and its surroundings.

In principle, however, we can overcome this difficulty by the following definition of the Peclet number:

$$\rho_i = \lim_{\substack{V_i \to 0 \\ (n \to \infty)}} \frac{2V}{V_i}\frac{U_i}{T_i}. \qquad [32]$$

As mentioned above, when approaching the limit of an infinite number of vessels, the turnover rate increases to infinity, but V_iT_i remains finite. While the definition [32] can be considered model-free, a numerical evaluation of ρ_i requires formidable numerical work, which becomes more and more inaccurate as the number n increases, even if we can assume that concentration curves are available for the entire system.

Let us return to the one dimensional diffusional flow system, where we take a model of n stirred tanks (figure 3) having equal volumes. When $n \to \infty$, $W_1 \to W_2$ and $T_i = 2W_1 = 2W_2$. It can be shown that the mixing rate can be represented then by:

$$T_i = 2W_1 = 2W_2 = 2nD_iA/L$$

(see also section 6). Equation [32] yields then the following expression for ρ_i:

$$\rho_i = \frac{U_iL}{\underset{n\to\infty}{AD_i}} \qquad [33]$$

which is similar to the "usual" Peclet number. In the simple case described by [26]–[27] and figure 3, $U_i = W$. In other cases, however, the purging rate is a local property and [33] can be regarded as an extension of the definition of the Peclet number.

5. SOJOURN TIME DISTRIBUTIONS AND ESCAPE PROBABILITIES

In section 2 we have treated the transition probabilities between different points. These are used in this section for the definition of several sojourn time distributions which, similar to the residence time distribution, provide some insight to the underlying transport processes in flow systems and are more amenable to physical interpretation. We are especially interested in sojourn time distributions which can be measured in a direct way without complex computations.

Let us first consider the system with a single inlet and a single outlet. Introducing an amount m of tracer as a pulse at the inlet and measuring the resulting concentration history at the outlet, the residence time distribution is directly obtained. The probability density $f(t)$ for residence time t is given by:

$$f(t) = \frac{c_e(t)}{\int_0^\infty c_e(t)\,dt} = \frac{W}{m} c_e(t) \qquad [34]$$

where use was made of [16]. The average residence time is related to the volume of the system by:

$$\bar{t} = \int_0^\infty t f(t)\,dt = \frac{W}{m}\int_0^\infty t c_e(t)\,dt = \frac{V}{W}. \qquad [35]$$

In many cases there is a considerable weight in the tail of the distribution (large values of t), where it is difficult to measure $f(t)$. It was already shown by Naor & Shinnar (1963) that the information obtained can be considerably improved by additional experiments. Injecting tracer in the inlet (f) and measuring at any point i in the system gives the local age distribution $a_i(t)$ at i:

$$a_i(t) = \frac{c_{fi}(t)}{\int_0^\infty c_{fi}(t)\,dt} = \frac{W^f}{m} c_{fi}(t). \qquad [36]$$

Similarly, injecting at i and measuring at the outlet e, the remaining life (or the "anti-age") distribution is found by:

$$b_i(t) = \frac{c_{ie}(t)}{\int_0^\infty c_{ie}(t)\,dt} = \frac{W^e}{m} c_{ie}(t). \qquad [37]$$

For systems having more than one inlet or outlet, a residence time distribution cannot be defined clearly and has no meaning. Other sojourn time distributions can be used then to characterize the system, namely, age and remaining life distributions. These can be defined for the entire system (as the distributions for a particle taken at random from the system at large). They are more significant, however, as local properties and their spatial distribution can yield information about mixing processes and interaction between regions (e.g. stagnancy, by-passing).

Obviously, an experiment in which tracer is injected (as a pulse) at one point i and the concentration $c_{ij}(t)$ is measured at point j yields directly the age distribution between these points. The probability density $\alpha_{ij}(t)$ for age t of a particle at j that entered the system at i, is given by:

$$\alpha_{ij} = \frac{c_{ij}(t)}{\int_0^\infty c_{ij}(t)\,dt} = \frac{p_{ij}(t)}{\int_0^\infty p_{ij}(t)\,dt}. \qquad [38]$$

A sojourn time distribution which is often more interesting than the age is that of the local remaining life distribution. The latter is useful in comparing the flow patterns of different regions

of the system, like purging and back-mixing. Higher average remaining life, for example, implies a tendency to stagnancy.

For any system, the probability density $b_i(t)$ for local remaining life distribution (at any point i) can be obtained by injecting the tracer there and measuring over all the system. $b_i(t)$ can be derived from the measurement without fitting to any model. It will be shown that $b_i(t)$ is given by:

$$b_i(t) = -\frac{1}{m}\frac{\mathrm{d}}{\mathrm{d}t}\sum_k c_{ik}(t)V_k = -\frac{1}{m}\frac{\mathrm{d}}{\mathrm{d}t}M(t). \qquad [39]$$

In some cases the total amount of tracer $M(t)$ within the system can be directly measured (not via concentration measurements). Such experiments are used in physiology, where the total count of radioactive tracers is recorded for a whole organ. In these cases the remaining life distribution is directly obtained (model-free) from the measurement, using [39]. When the system is closed M is constant and the probability density b_1 is trivially zero.

Let us now discuss the definition of the age and remaining life distributions on the basis of compartmental analysis, bearing in mind that a continuous system can be described by a network in which the number of vessels tends to infinity. We derive first, the local age distribution $a_j(t)$ for a random particle at j, that is, a particle at j which could enter the system through any inlet. The probability Q_{ij}^f that a particle at j has entered the system at the inlet to vessel i is given by:

$$Q_{ij}^f = \frac{W_i^f\int_0^\infty p_{ij}\,\mathrm{d}t}{\sum_i W_i^f\int_0^\infty p_{ij}\,\mathrm{d}t} = \frac{W_i^f}{V_j}\int_0^\infty p_{ij}\,\mathrm{d}t = \frac{W_i^f P_{ij}}{\sum_i W_i^f P_{ij}}, \qquad [40]$$

where use has been made of [12] and [19]. The probability density $\alpha_{ij}(t)$ for age t of a particle at j that entered the system through i is given by [38]. Thus the probability density $a_j(t)$ for age t of a random particle at j is:

$$a_j(t) = \sum_i Q_{ij}^f\alpha_{ij}(t) = \frac{1}{V_j}\sum_i W_i^f p_{ij} = \frac{1}{m}\sum_i w_i^f c_{ij}(t), \qquad [41]$$

and [36] is obtained as a special case for a single inlet system. The probability density $a(t)$ for age t for a random particle in the entire system is given by:

$$a(t) = \frac{\sum_j V_j a_j(t)}{\sum_j V_j} = \frac{1}{V}\sum_i\sum_j W_i^f p_{ij}(t). \qquad [42]$$

The age distribution for any subsystem can also be calculated by [42], where the summation of the inflows W_i^f includes all the inflows into this subsystem from all other regions of the system.

We can define now the age distribution at the outlet of the system, regarding all the outlets as a common one:

$$a^e(t) = \frac{\sum_j w_j^e a_j(t)}{\sum_j w_j^e}. \qquad [43]$$

Let us now derive some expressions for the remaining life distributions. The probability that a particle at i will leave the system through the outlet of vessel j is $p_{ij}^e(\infty)$.

The probability density $\beta_{ij}(t)$ for remaining life t of a particle at i which will leave the system

through j is:

$$\beta_{ij}(t) = \frac{1}{p^e_{ij}(\infty)} \frac{dp^e_{ij}(t)}{dt} \qquad [44]$$

and the probability density $b_i(t)$ for remaining life t of a random particle as i is:

$$b_i(t) = \sum_j p^e_{ij}(\infty)\beta_{ij}(t) = \sum_j \frac{dp^e_{ij}(t)}{dt} = \sum_j w_j{}^e p_{ij}(t) = \frac{1}{m} \sum_j w_j{}^e c_{ij}(t) \qquad [45]$$

where use was made of [5] and [7]. From [45] another form for $b_i(t)$ can be obtained:

$$b_i(t) = \frac{d}{dt} \sum_j p^e_{ij}(t) = \frac{d}{dt} \left[1 - \sum_k p_{ik}(t) \right] \qquad [46]$$

which follows from the fact that the sum of all the transition probabilities from any point (to all points within the system and the outlets) is unity. Introducing [5] into [46], the probability density $b_i(t)$ reduces to the form [39] which is directly measurable. Finally, the remaining life distribution for a random particle at the inlet (when regarding all the inlets as a common one) is:

$$b^f(t) = \frac{\sum_i w_i{}^f b_i(t)}{\sum_i w_i{}^f}. \qquad [47]$$

Both the age distribution at the outlet [43] and the remaining life at the inlet [47] can be defined as an equivalent residence time distribution, and from [41] and [45] it can be shown that:

$$a^e(t) = b^f(t). \qquad [48]$$

Usually, a residence time distribution is meaningful for systems of single inlet–single outlet. However, in many cases the boundaries of the system cannot be clearly defined (as in the case of some estuaries). For such cases and for systems having multiple inlets and outlets, local remaining life distributions can serve to compare the nature of the purging and mixing processes of various regions, and an equivalent residence time distribution as defined by [43] or [47] can describe the system as a whole.

Measuring $b(t)$ or $a(t)$ in a system with multiple inlets and outlets involves measurement of the total amounts of tracer in the system. Since this is often difficult, we need sojourn time distributions that can be obtained from more limited measurements, either at the point of injection or in another given region.

Let us first consider the case where $i = j$. For this case we can define a properly normalized probability density:†

$$\pi_{ii}(t) = \frac{p_{ii}(t)}{\int_0^\infty p_{ii}(t)\,dt} = \frac{U_i}{V_i} p_{ii}(t) = \frac{U_i c_{ii}(t)}{m}, \qquad [49]$$

where use was made of [18].

†In a closed system the integral of p_{ij} is infinite and there is no way to obtain a proper probability density. Naor *et al.* (1972) showed that some more general distribution functions (extended distributions) can be observed for that specific case, which contains considerable information about the mixing process. However, if there are one or more inlets (and, therefore, in steady state also an outlet) the integral of p_{ij} is finite and in this case we can normalize it to a proper probability density function.

Expression [49] resembles a regular residence or remaining life distribution, using U_i as the flow rate. $\pi_{ii}(t)\,dt$ is the probability to leave (for the last time) the influence sphere of vessel i at time t, given that at time zero the particle was in i. This does not mean that it stays in vessel i all the time: it could leave and come back many times before t. The influence sphere is not a clearly defined physical region but rather a region in an imaginary space related to the effect of the mixing processes on the probability of a particle to return to i before leaving the system.

π_{ii} is a proper probability density and its advantage is the same as for regular residence or remaining life distributions. Namely, it presents the information in a way which is easy to interpret physically. Thus, for example, multiple peaks in π_{ii} imply recirculation. We can also compute the escape probability:

$$\eta_{ii}(t) = \frac{\pi_{ii}(t)}{1 - \int_0^t \pi_{ii}\,dt}, \qquad [50]$$

which provides, again, insight into the physical processes underlying the mixing.

Let us now turn to the case where i is not equal to j. The probability of a particle which is initially at vessel i to reach j between t and $t+dt$ is $\alpha_{ij}(t)\,dt$ where α_{ij} is given by [38]. This probability contains very little information; however, when combined with the probability P_{ij} [19], obtained by a single additional experiment of injecting and measuring at j, much more information can be learned. We define the following extended probability density:

$$\pi_{ij}(t) \equiv \frac{U_j c_{ij}(t)}{m} = \frac{p_{ij}(t)P_{ij}}{\int_0^\infty p_{ij}(t)\,dt} = \alpha_{ij}(t)P_{ij}, \qquad [51]$$

$\pi_{ij}dt$ is the probability that a particle which at time zero is in i, will leave the influence sphere of j at time t.

Both π_{ij} and P_{ij} give important clues for an appropriate flow model. For example, in a system with a single outlet, even if there is backflow through this outlet, P_{ij} is unity if j is near the outlet. Therefore, a measurement in j gives a proper net outflow and π_{ij} can be evaluated as a remaining life distribution.

6. APPLICATION TO CONTINUOUS FLOWS—AN EXAMPLE OF A TWO-PHASE FLOW

In the previous sections we have discussed the use of tracers to investigate mixing processes in flow systems from two different approaches. One is the estimation of model parameters from the results of tracer experiments. This approach is useful when we have a good knowledge of the underlying transport processes and can, therefore, set up a reasonable model.

The second approach is the evaluation of model-free parameters which are directly obtained from the measurements. In this way we can learn about the behavior of the system regardless of any model; moreover, we can gain information about the reliability of models describing the system or get a better feeling as to what a suitable model should be.

The definitions of such model free parameters as the local purging rate, the remaining life distribution and in principle the local Peclet number, were based on compartmental analysis. However, as mentioned on several occasions through this article, the methods discussed here are mainly intended and apply to continuous systems.

In this section we treat an example of a tracer experiment in a continuous system and discuss the application of the two approaches to it. Consider the system described in figure 6. The flow system consists of two phases: I is a well mixed vessel having volume V and a net flow rate W through it; II is a one-dimensional diffusional component, having diffusion coefficient D, cross-section area A and length L: phase II is well mixed normal to the direction of Z. The two phases are coupled via a mass transfer coefficient h. This case was treated by Shinnar *et al.* (1972)

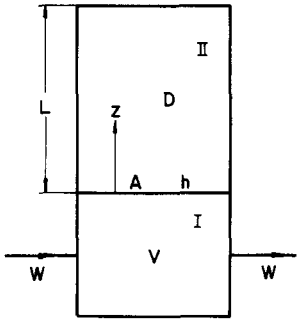

Figure 6. Two-phase flow—a diffusional model.

and we briefly recount their solution. The equations and boundary conditions for an experiment in which an amount m of tracer is injected as a pulse at time $t = 0$ at phase I are:

$$\frac{\partial c_{II}(Z,t)}{\partial t} = D\frac{\partial^2 c_{II}(Z,t)}{\partial z^2} \qquad 0 \leqslant Z \leqslant L, \qquad [52a]$$

$$\frac{\partial c_{II}(L,t)}{\partial Z} = 0, \qquad [52b]$$

$$-D\frac{\partial c_{II}(0,t)}{\partial Z} = h[c_I(t) - c_{II}(0,t)], \qquad [52c]$$

$$V\frac{dc_I(t)}{dt} = -Wc_I(t) + hA[c_{II}(0,t) - c_I(t)], \qquad [52d]$$

$$c_I(0) = \frac{m}{V}, \qquad [52e]$$

$$c_{II}(Z,0) = 0 \qquad 0 \leqslant Z \leqslant L. \qquad [52f]$$

The above equations can be solved to yield the concentrations $c_{II}(Z,t)$ and $c_I(t)$; the latter is also equal to the concentration at the outlet. Some curves of $c_I(t)$ are plotted in figure 7, where η and ξ are defined in [54].

We can now ask what would we learn from additional experiments. For our purpose the Laplace transforms $\hat{c}_I(s)$ and $\hat{c}_{II}(Z,s)$ of the concentrations at I and II (respectively) contain sufficient information and we do not need the complete solutions of $c_I(t)$ and $c_{II}(Z,t)$. The

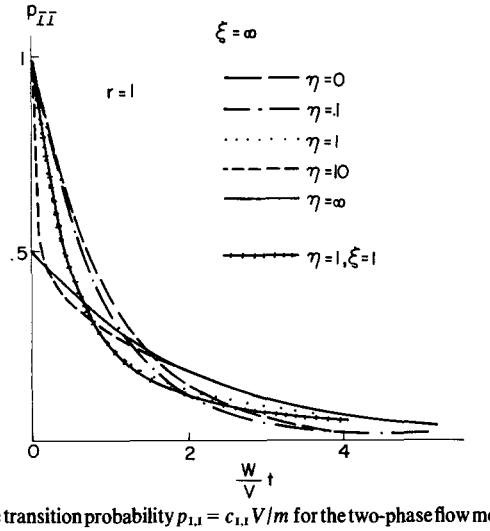

Figure 7. The transition probability $p_{I,I} = c_{I,I}V/m$ for the two-phase flow model (figure 6).

solutions for $\hat{c}_{\mathrm{I}}(s)$ and $\hat{c}_{\mathrm{II}}(Z, s)$ for injection at the inlet are given by the following dimensionless form:

$$f_{\mathrm{II}}(s) = \frac{W}{m}\hat{c}_{\mathrm{I}}(s) = \left[1 + s + \xi\sqrt{[(r/\xi)s]} - \frac{\tanh\sqrt{[(r/\xi)s]}}{1 + \frac{\xi}{\eta}\tanh\sqrt{[(r/\xi)s]}}\right]^{-1}, \qquad [53a]$$

$$\frac{W}{m}\hat{c}_{\mathrm{II}}(s) = \frac{\exp(\sqrt{[(r/\xi)s]}) - \exp[\sqrt{[(r/\xi)s]}(2-z)]}{1 + s - \dfrac{(1/\xi)\sqrt{(r/\xi)}[1-\exp(2\sqrt{(r/\xi)})]}{1+\exp[2\sqrt{(r/\xi)}] - (\xi/\eta)[1-\exp(2\sqrt{(r/\xi)})]}}, \qquad [53b]$$

where

$$z = \frac{Z}{L}; \quad r = \frac{LA}{V}; \quad \xi = \frac{DA}{WL}; \quad \eta = \frac{hA}{W} \qquad [54]$$

and s is based on $t^* = (W/V)t$. The zeroth moment of the concentration at phase I yields the flow rate W, as can be seen from [53a]:

$$(\mu_{\mathrm{I}})_0 = \int_0^\infty c_{\mathrm{I}}\,\mathrm{d}t = \lim_{s\to\infty}\hat{c}_{\mathrm{I}}(s) = \frac{m}{W}, \qquad [55a]$$

which is an obvious result.

As mentioned above, an accurate measurement of c_{I} would theoretically allow determination of h, D and W. As the first moment is simply the average residence time, we need the second and third moments to estimate h and D:

$$\frac{W}{m}(\mu_{\mathrm{I}})_1 = (V + LA)/W = \frac{V}{W}(1 + r) = \bar{t}, \qquad [55b]$$

$$\frac{W}{m}(\mu_{\mathrm{I}})_2 = \left(\frac{V}{W}\right)^2\left[2(1+r)^2 + 2\frac{r^2}{\eta} + \frac{r}{3}\frac{r^2}{\xi}\right] = \sigma^2 + (\bar{t})^2, \qquad [55c]$$

$$\frac{W}{m}(\mu_{\mathrm{I}})_3 = \left(\frac{V}{W}\right)^3\left[6(1+r)^3 + 12r^2(1+r)\left(\frac{1}{\eta} + \frac{1}{3\xi}\right) + r^3\left(\frac{6}{\eta^2} + \frac{4}{\xi\eta} + \frac{4}{5}\frac{1}{\xi^2}\right)\right]. \qquad [55d]$$

The difficulty is that $(\mu_{\mathrm{I}})_2$, $(\mu_{\mathrm{I}})_3$, and even $(\mu_{\mathrm{I}})_1$ are hard to measure accurately, especially if h or D are very small or very large. Indeed, from figure 7 it can be seen that the curve of $f(t)$ for $\eta = 0$ is indistinguishable from that for $\eta = 0.1$, and the same is true for any curve where $\eta > 10$. In the latter case the system is nearly a stirred tank and we can get very little help from additional experiments.

The zeroth moment of the response in phase II at any point z will give, again, m/W. The first moment is:

$$\frac{W}{m}(\mu_{\mathrm{II}})_1 = \frac{V}{W}\left[(1+r) + \frac{r}{2\eta} + \frac{r}{4\xi}z\right]. \qquad [56]$$

Thus, two measurements at different points in phase II can yield both h and D from the first moment, which is easier to measure than higher moments.

If h is small this method will not work as $c_{\mathrm{II}}(t)$ will be too small. In this case an additional injection in II followed by a measurement in II will give the desired parameters more accessibly. In order to find the response to such an injection, we have to solve equations [52] with the initial conditions:

$$c_{\mathrm{I}}(0) = 0, \qquad [57a]$$

$$c_{II}(z, 0) = \frac{m}{A}\,\delta(z_0) \qquad [57b]$$

where $\delta(\ )$ is the Dirac delta function.

Again, we need only the Laplace transforms $\hat{c}_I(s)$ and $\hat{c}_{II}(z, s)$ which are given by:

$$\frac{W}{m}\,\hat{c}_{II}(z, s) = \begin{cases} Y_3 \exp(\sqrt{[(r/\xi)]}z) + Y_4 \exp(-\sqrt{[(r/\xi)]}z) & 0 \leq z \leq z_0 \\ Y_1 \exp(\sqrt{[(r/\xi)]}z) + Y_2 \exp(-\sqrt{[(r/\xi)]}z) & z_0 \leq z \leq 1, \end{cases} \qquad [58a]$$

$$\frac{W}{m}\hat{c}_I(s) = Y_3 + Y_4 - \frac{\xi}{\eta}\sqrt{(r/\xi)}(Y_3 - Y_4) \qquad [58b]$$

where:

$$Y_3 = \frac{\psi[(1+s)(1+(\xi/\eta)\sqrt{[(r/\xi)]}) + \xi\sqrt{[(r/\xi)]}]}{(1+s)\{1+\exp(2\sqrt{[(r/\xi)]}) - (\xi/\eta)\sqrt{[(r/\xi)]}[1-\exp(2\sqrt{[(r/\xi)]})]\}}, \qquad [59a]$$

$$Y_4 = Y_3 \exp(2\sqrt{[(r/\xi)]}) - \psi, \qquad [59b]$$

$$Y_1 = Y_3 - \frac{1}{2}\frac{1}{\xi\sqrt{[(r/\xi)]}}\exp(-\sqrt{[(r/\xi)]}z_0), \qquad [59c]$$

$$Y_2 = Y_1 \exp(2\sqrt{[(r/\xi)]}), \qquad [59d]$$

$$\psi = \frac{1}{2}\frac{1}{\xi[(r/\xi)]}\{\exp(\sqrt{[(r/\xi)]}z_0) + \exp[2\sqrt{[(r/\xi)]}(2 - z_0)]\}. \qquad [59e]$$

From the above solution the zeroth moment of the concentration $c_{III}(t)$ at any point $0 \leq z \leq z_0$ is found to be:

$$\int_0^\infty c_{III}(z, t)\,dt = \lim_{s\to\infty} \hat{c}_{II}(z, s) = \frac{m}{W}\left(1 + \frac{1}{\eta} + \frac{z}{\xi}\right) \quad 0 \leq z \leq z_0. \qquad [60a]$$

The first moment at $z = z_0$ is given by:

$$\int_0^\infty t\,c_{III}(z, t)\,dt = \frac{m}{W}\frac{V}{W}\left[(1+r) + \frac{r}{\eta} + \frac{r}{\xi}z_0\left(1 - \frac{1}{2}z_0\right) - \frac{2(\xi/\eta) + rz_0 + 2z_0 + (1/6)(r/\xi)z_0^3 + (r/\eta)z_0^2}{2((\xi/\eta) + \xi + z_0)}\right]. \qquad [60b]$$

Thus, the parameters h and D can also be estimated from the zeroth and first moments of the response $c_{III}(z, t)$. Measurements at several points in II yield all the information from the zeroth moment only. As mentioned before, the accuracy is then much higher. From the curves of the concentration histories $c_{III}(t)$ and $c_{II}(t)$ in figures 8 and 9, it can be seen that the difference between curves for various values of η (especially for small η) is much larger than for the inlet–outlet experiment (figure 7).

Let us now evaluate the local purging rates, Peclet numbers, and remaining life distributions in the system described by figure 6.

The purging rate in phase I (the mixed vessel) is, according to the definition [20], equal to the flow rate W:

$$U_I = W \qquad [61]$$

because the probability of a particle at the (single) inlet to pass through phase I is unity. In phase II the purging rate U_{II} varies along the distance z. It can be measured directly by injecting tracer

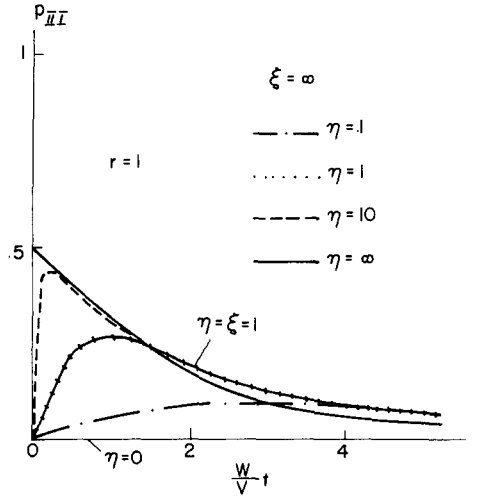

Figure 8. The transition probability $p_{II,I} = c_{II,I}V/m$ for the two-phase flow model (figure 6).

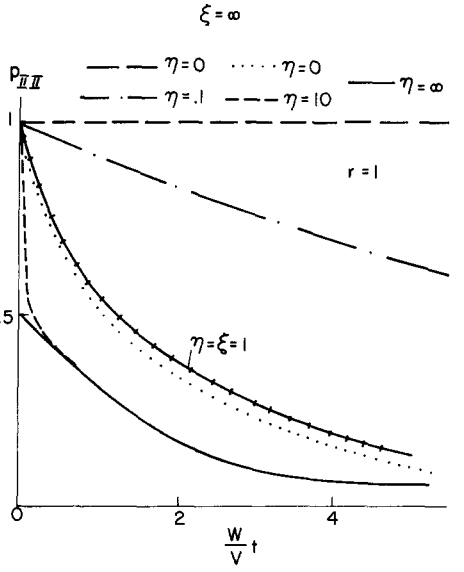

Figure 9. The transition probability $p_{II,II} = c_{II,II}LA/m$ for the two-phase flow model (figure 6).

at any point z and recording the resulting concentration history there (see [17]):

$$U_{II}(z_0) = \frac{m}{\int_0^\infty c_{II}(z_0, t)\,dt}. \qquad [62]$$

In order to obtain the variation of U_{II} as a function of z, many such experiments have to be carried out. If the system parameters are known, the purging rate $U_{II}(z)$ can be calculated by [62] and [60] using the fact that z_0 is arbitrary and, therefore, can be replaced by z:

$$\frac{U_{II}(z)}{W} = \frac{1}{1 + \frac{W}{hA} + \frac{Wz}{DA}} = \frac{1}{1 + \frac{1}{\eta} + \frac{1}{\xi}z}. \qquad [63]$$

Thus, from the measurements of the purging rates in phase II, the system parameters can be evaluated.

The variation of the purging rate in phase II is shown in figure 10.

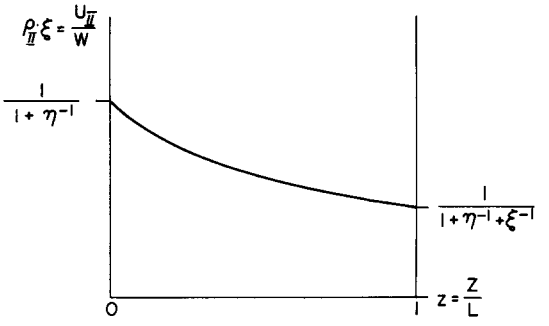

Figure 10. Variation of the purging rate and the Peclet number along Phase II.

Several special cases are of interest. Consider first the case where both h and D tend to infinity. Both phases then become together a single well-mixed vessel and the purging rate tends to W.

When $D \to \infty$ but h is infinite, phase II becomes a well-mixed vessel and the purging rate is then uniform:

$$\frac{U_{II}}{W} = \frac{1}{1+\frac{1}{\eta}}. \qquad [64]$$

Finally, when D is finite and h tends to infinity, the purging rate reduces to:

$$\frac{U_{II}(z)}{W} = \frac{1}{1+\frac{Wz}{AD}} = \frac{1}{1+\frac{z}{\xi}} \qquad [65]$$

and there is no abrupt change of U across the surface between the phases.

The equivalent Peclet number $\rho(z)$ at any point z is found from [33]:

$$\rho(z) = \frac{U(z)L}{AD} = \frac{1}{\xi\left(1+\frac{1}{\eta}+\frac{1}{\xi}z\right)}. \qquad [66]$$

The curve in figure 10 describes, then, also the variation of $\rho(z)$ (when scaled properly by ξ).

The local remaining life distribution $b_i(t)$ at any point can be obtained by injecting the tracer there and measuring at the outlet (or phase I) or by measuring everywhere (see section 5). For phase I, $b_i(t)$ is identical with the residence time distribution as explained above:

$$f(t) = b_I(t) = \frac{W}{m} c_{I,I}(t). \qquad [67]$$

The average and variance of the distribution are given by [55b] and [55c].

The local probability density for remaining life for phase II is given by:

$$b(z,t) = \frac{W}{m} c_{zI}(t). \qquad [68]$$

Thus, the curves of $c_{II}(t)$ in figure 8 also express the remaining life distributions (when scaled properly).

Using [58] and [59], the following is obtained for the average and variance of $b(z,t)$:

$$\bar{t}_{(b)}(z) = \frac{V}{W}\left[(1+r)+\frac{r}{\eta}+\frac{r}{\xi}\left(z-\frac{z^2}{2}\right)\right], \qquad [69]$$

$$\sigma_b^2 = \left(\frac{V}{W}\right)^2\left\{(1+r)^2+2\frac{r^2}{\eta}+\frac{2}{3}\frac{r^2}{\xi}-\frac{2}{3}\left(\frac{r}{\xi}\right)^2+\frac{2}{3}\frac{r^2}{\xi\eta}+\frac{1}{24}\left(\frac{r}{\xi}\right)^2[z^2+(2-z)^2]+\left(\frac{r}{\xi}\right)^2\left(z-\frac{1}{2}z^2\right)\right.$$
$$\left.\times\left(2-z+\frac{1}{2}z^2\right)\right\}. \qquad [70]$$

It can be seen, again, that when there are no resistances ($\eta, \xi \to \infty$) the system can be considered as one mixed vessel and the remaining life distribution for II becomes equal to the residence time distribution.

Let us discuss now the problem of interpreting the results of tracer experiments in the system when we have no *a priori* knowledge about the nature of the flow in it. The model-free parameters defined in the previous sections are useful then. Suppose that we can perform several experiments in which tracer is injected at any point (i) and the resulting concentration history is measured there. The local purging rates U_i and the local sojourn time distributions $\pi_{ii}(t)$ are then directly obtained from the measurements, by [17] and [49].

Valuable information about the system is gained from the spatial distribution of U_i (and π_{ii}). For example, uniformly of the purging rate in region I implies that it can be considered as a mixed vessel; if U is equal to the total inflow rate W (measured by the inlet–outlet response), then all the flow passes through I and there is no parallel flow through II only. The fact that I is well mixed can also be discovered by the uniformity of the responses there to injection of tracer at II.

If the purging rates at phase II are found to be uniform laterally (at points with the same z), the assumption of strong mixing in that direction is justified. An abrupt change (discontinuity) of U indicates a strong resistance which may be due to an inter-phase surface.

The local transition probability of π_{jj} (see section 5) contains some additional important information. Just the fact that it is monotonous shows that there are no recirculation processes in phase II and as $U(z)$ decreases with z, a diffusional process might be a suitable model.

Similar conclusions can be deduced from the local remaining-life distributions obtained by injecting at these points and measuring at the outlet (see section 5).

It is noted that such detailed results cannot be obtained by the simple experiment of injecting at the inlet and measuring at the outlet. For example, the residence time distribution might detect several types of stagnancies, especially by the behavior of the tail. However, very small and very large stagnancies are hard to detect in this experiment: the former because its effect will be negligible at the outlet, and the latter because the time scale of all the experiment is smaller than that for the stagnancy.

The equivalence of compartmental and diffusional models

Until now we have described the system by a diffusional flow model governed by [52]. There is, however, one serious disadvantage in this representation: partial differential equations are much harder to solve when dealing with complex chemical reactions or other added processes such as coalescence. In these cases we would prefer simple flow models consisting of a network of a small number of well-mixed vessels which contain all the basic physics of the real flow.

To find such a proper model for the flow given by [52] we can choose the network described in figure 11 and the problem is to find the number of mixed vessels as well as the connecting flowrates. We can do this by demanding that each vessel will have all the local mixing properties of the real flow; namely, the same purging rate and the same local Peclet number.

The flow rate W_1 is determined by the condition that it will be equal to the rate of interchange at the interface:

$$W_1 = hA. \qquad [71]$$

The other flow rates W_j are free parameters as are the volumes $V_j (j = 1, 2, \ldots, n)$.

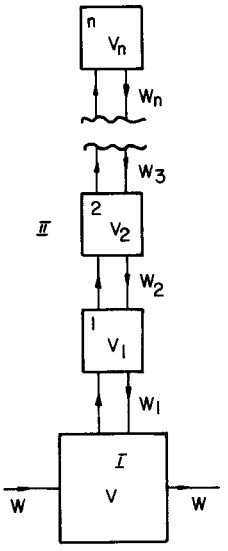

Figure 11. A model of well-stirred tanks representing the two-phase flow of figure 6.

The purging rate U_i in vessel i is found from [20]:

$$U_i = WP_{1i} \tag{72}$$

where

$$P_{1i} = P_{11}P_{12}P_{23}\ldots P_{i-1,i} \tag{73}$$

is the probability of a particle at I to pass through vessel i. The first two probabilities are given by:

$$P_{11} = W_1/(W + W_1), \tag{74a}$$

$$P_{12} = W_2\Big/\left[W_1 + W_2 - \frac{W_1^2}{W_1 + W}\right] \tag{74b}$$

and the probability $P_{i-1,i}$ is:

$$P_{i-1,i} = \left[1 + \frac{W_{i-1}}{W_i}(1 - P_{i-2,i-1})\right]^{-1}. \tag{74c}$$

Thus, the purging rate at vessel i [72] depends on all the flow rates connecting the vessels between I and i.

If all the flow rates W_j are taken to be the same (and equal to W_2), [74c] reduces to:

$$P_{i-1,i} = \frac{1}{2 - P_{i-2,i-1}}, \tag{75}$$

and by a series of regressions, the produce $P_{23}P_{34}\ldots P_{i-1,i}$ can be expressed as follows:

$$P_{2i} = P_{23}P_{34}\ldots P_{i-1,i} = [i - 1 + (i-2)P_{12}]^{-1}. \tag{76}$$

Introducing [76] and [74b] into [72] the purging rate U_i is found to be:

$$U_i = \frac{W}{1 + \dfrac{W}{W_1} + (i-1)\dfrac{W}{W_2}}. \tag{77}$$

When increasing the number of vessels n indefinitely and approaching the limit of the continuous system described by [52], the flow rate W_2 becomes related to the diffusion coefficient D by:

$$W_2 = n\frac{AD}{L} \qquad [78]$$

(see also section 4). It is seen that the purging rate reduces then to that given by [63], where $z = (i-1)/n$.

The turnover rate at vessel i is, according to [25]:

$$T_i = W_i + W_{i+1}. \qquad [79]$$

Thus, the local Peclet number ρ_i for vessel i is given, according to [31], by:

$$\rho_i = \frac{2LA}{V_i}\frac{U_i}{W_i + W_{i+1}} \qquad [80]$$

where U_i is given by [72]. When all the flow rates $W_j (j \geq 2)$ are equal to W_2 the purging rate is given by [77] and the Peclet number is:

$$\rho_i = \frac{LA}{V_i}\left[\frac{W_2}{W}\left(1 + \frac{W}{W_1} + (i-1)\frac{W}{W_2}\right)\right]^{-1}. \qquad [81]$$

The limit of $n \to \infty$ leads to the continuous diffusional description. Taking then vessels of equal volumes, $LA/V_i = n$, and introducing [71] and [78] into [81], the local Peclet number reduces, indeed, to the form [66].

We have concluded that the model of a cascaded network of mixed vessels can represent the diffusional flow: when the number of vessels tends to infinity both the local purging rate and the local Peclet number approach the proper limit.

Moreover, for a large number of vessels, the Peclet number ([81] or [66]) has exactly the same form as the purging rate ([77] or [63]) except for a constant factor. It means that for large n, by choosing W_2 to fit the spatial distribution of the purging rate within a certain accuracy limit, the local Peclet number at each vessel is determined within the same limit.

For a model consisting of a small number of vessels, n is determined by the desired accuracy limit and the maximum relative variation of the purging rate $(U(0) - U(L))/U(L)$, or that of the Peclet number (usually by the former which is more directly accessible from measurements). An optional method for the modelling is letting W_i and V_i vary and estimating them by fitting with the measured U_i within the desired accuracy limit. Because of the close resemblance between the forms of U_j and ρ_i, the deviations in the latter will not be much larger. However, as shown in the following example, even if we choose equal-size vessels and allow only W_i to change, the results for the purging rates and the Peclet numbers agree with those of the continuous system quite well.

The accuracy reached by the same model for the average and variance of the local remaining-life distribution is higher than for U and ρ, because the details of the modelling in phase II have less effect on the response at the outlet. The residence time distribution (given by the response at the outlet to injection at the inlet) is even less affected by these details.

As an example we choose 4 vessels of equal volume to represent phase II for the case $\eta = \xi = 1$, $r = 1$. In this example the purging rate U_i is fitted to $U(z)$ from [62] at the center of each vessel, and W_j is determined by [72]–[74]. The results are listed in table 2, which also includes the results for the Peclet numbers and the remaining life distributions. From the results it can be seen that a model of four equal-sized vessels represents the continuous system within a

Table 2. Modelling the continuous system with $r = 1$, $\xi = 1$ and $\eta = 1$ by four mixed vessels (see figure 11)

$z = \frac{Z}{L}$	0	(0.125)	0.25	(0.375)	0.50	(0.625)	0.75	(0.875)	1
i		1		2		3		4	
$U(z)/W = \rho(z)$	0.5	0.470	0.445	0.421	0.40	0.381	0.363	0.348	0.333
U_i/W		0.470		0.421		0.381		0.348	
W_i/W		0.890		4.05		4.01		4.09	
Max. deviation in U		6.0%		5.4%		5.0%		4.5%	
ρ_i		0.464		0.418		0.376		0.340	
Max. deviation in ρ		7.2%		6.1%		6.0%		6.3%	
$\frac{W}{V}\bar{t}_{(b)}(z)$	3.0		3.22		3.37		3.47		3.50
$\frac{W}{V}(\bar{t}_b)_i$		3.12		3.31		3.43		3.49	
Max. deviation in $\bar{t}_b$		4%		2.8%		1.8%		< 1%	
$\gamma^2(z) = \sigma_b^2(z)/(\bar{t}_b)^2$	0.92		0.81		0.75		0.71		0.69
$(\gamma_b^2)_i$		0.86		0.78		0.73		0.70	
Max. deviation in γ_b^2		6.5%		4.0%		2.8%		1.4%	

$\frac{W}{V}\bar{t}_{(f)} = 2$; $\gamma_f^2 = 1.66$ (continuous system); $\gamma_f^2 = 1.67$ (model)

very reasonable accuracy. Also, it can be seen that the values of W_2 are very close, which indicates that a model of equal-sized vessels with equal inter-flow rates will be a good approximation for any practical application.

REFERENCES

ARIS, R. 1966 Compartmental analysis and the theory of residence time distribution. In *Intracellular Transport* (Edited by WARREN, K. B.) p. 167. Academic Press, New York.

BARRETT, M. A., MUNRO, D. & AGG, A. R. 1969 Radiotracer dispersion studies in the vicinity of a sea outfall. *Adv. Water Pollution Res.* **6**, 863–876.

BASSINGTHWAIGHTE, J. B. 1974 Personal communication.

BERGNER, P-E., E. 1961 Tracer dynamics: 1. A tentative approach and definition of fundamental concepts. *J. theor. Biol.* **2**, 120–140.

CANNON, P. J., DELL, R. B. & DWYER, E. M. JR. 1972 Measurement of regional myocardium perfusion in man with ^{133}Xenon and a scintillation camera. *J. clin. Invest.* **51**, 964–977.

CEDERWALL, F. & HANSEN, J. 1968 Tracer studies on dilution and residence time distribution in receiving waters. *Water Res.* **2**, 297–310.

CLAYTON, C. G. & SMITH, D. B. 1963 A comparison of radioisotrope methods for river flow measurements. In *Radioisotopes in Hydrology*. Int. Atomic Energy Agency, Vienna.

DINGER, T. 1967 Application of radiotracer methods in streamflow measurements. In *Isotopes in Hydrology*. Int. Atomic Energy Agency, Vienna.

DUANE, D. B. 1970 Tracing Sand Movement in the Littoral Zone: Progress in the Radioisotopic Sand Tracer (RIST) Study, July 1968–February 1969. U.S. Army Corps of Engineers, Coastal Engineering Research Center, Miscellaneous Paper No. 9–70, August 1970.

GRAUPE, D. 1972 *Identification of Systems*. Van-Nostrand, Reinhold.

HARLEMAN, D. R. F., HOLLEY, E. R. & HABER, W. L. 1966 Interpretation of water pollution data from tidal estuary models. *Adv. Water Pollution Res.* **3**, 49–64.

HARREMOES, P. 1966 Tracer studies on jet diffusion and stratified dispersion. *Adv. Water Pollution Res.* **3**, 65–85.

HART, H. E. 1960 Analysis of tracer experiments, IV. The kinetics of general N-compartment systems. *Bull. Math. Biophys.* **22**, 41–52.

HART, H. E. 1963 An integral equation formulation of perturbation tracer analysis. In *Multicompartment Analysis of Tracer Experiments, Annals of the New York Academy of Science*, (Edited by WHIPPLE, H. E.) pp. 23–28.

HEARON, J. Z. 1963 Theorems of linear systems. In *Multicompartment Analysis of Tracer*

Experiments, Annals of the New York Academy of Science, (Edited by WHIPPLE, H. E.) pp. 36–68.

INGRAM, W. T. & MITWALLY, H. 1966 Paths of pollution in New York Harbor: a model study. *J. Water Pollut. Control Fed.* (WPCF) **34**, 1563–1581.

KRAMBECK, F. J., KATZ, S. & SHINNAR, R. 1969 Interpretation of tracer experiments in systems with fluctuating throughput. *IEC Fundamentals* **8**, 431–441.

KRAMBECK, F. J., KATZ, S. & SHINNAR, R. 1969 A stochastic model for fluidized beds. *Chem. Engng Sci.* **24**, 1497–1511.

NAOR, P. & SHINNAR, R. 1963 Representation and evaluation of residence time distributions. *IEC Fundamentals* **2**, 278–286.

NAOR, P., SHINNAR, R. & KATZ, S. 1972 Indeterminacy in the estimation of flow rate and transport functions from tracer experiments in closed circulations. *Int. J. Engng Sci.* **10**, 1153–1174.

OBRIST, W. D., THOMPSON, H. K., KING, C. H. & WANG, H. S. 1967 Determination of regional cerebral blood flow by inhalation of ^{133}xenon. *Circulation Research* **20**, 124–135.

O'CONNOR, D. J. 1962 Organic pollution of New York Harbor—theoretical considerations. *J. Wat. Pollut. Control Fed.* **34**, 905–919.

O'CONNOR, D. J. 1966 An analysis of the dissolved oxygen distribution in the East river. *J. Wat. Pollut. Control Fed.* **38**, 1813–1830.

OKUBO, A. & PRITCHARD, D. W. 1969 Summary of Our Present Knowledge of the Physical Processes of Mixing in the Ocean and Coastal Waters. Chesapeake Bay Institute, The Johns Hopkins University, Report No. NYO-3109-40, Ref. 69–1.

SELLECK, R. E. & PEARSON, E. A. 1961 Tracer Studies and Pollutional Analysis of Estuaries. University of California, Berkeley, Sanitary Eng. Res. Lab.

SHINNAR, R. & NAOR, P. 1967 Residence time distributions in systems with internal reflux. *Chem. Engng Sci.* **22**, 1369–1381.

SHINNAR, R., NAOR, P. & KATZ, S. 1972 Interpretation and evaluation of multiple tracer experiments. *Chem. Engng Sci.* **27**, 1627–1642.

TSIVOGLOU, E. C., COHEN, J. B., SHEARER, S. D. & GODSIL, P. J. 1968 Tracer measurement of stream reaeration. II. Field studies. *J. Wat. Pollut. Control Fed.* **40**, 285–305.

ZIERLER, K. L. 1962 Circulation times and the theory of indicator-dilution methods for determining blood flow and volume. In *Handbook of Physiology*, Vol. 1, Section 2, *Circulation*, pp. 585–615, (Edited by HAMILTON, W. F. & DOW, P.). American Physiological Society, Washington D.C.

APPENDIX A: DETERMINATION OF THE $n \cdot n$ MATRIX OF FLOW RATES BY n TRACER MEASUREMENTS

Consider a tracer experiment in which tracer is injected into the qth vessel and concentration histories are recorded in all n vessels. The vector $\mathbf{p}_{(q)} = (p_{q1}, p_{q2}, \ldots, p_{qn})$ of transition probabilities [13]

$$p_{qi} = \sum_k A^k_{qi} e^{\lambda_k t} \qquad i = 1, 2, \ldots, n \qquad \text{[A-1]}$$

is then found. This means that in principle the eigenvalues $\lambda_1, \ldots, \lambda_n$ can be evaluated along with the n^2 coefficients A^k_{qi} $(i, k = 1, 2, \ldots, n)$. Using the definition [14] of A^k_{qi}, multiplying both sides by S^j_i and summing over the index i, the following is obtained:

$$\sum_i S^j_i A^k_{qi} = \sum_i S_q{}^k R^k_i S^j_i = \delta_{kj} S_q{}^k = \sum_i \delta_{iq} \delta_{kj} S^j_i \qquad \text{[A-2]}$$

where use was made of the orthonormality of $\mathbf{S}^k$ and $\mathbf{R}^j$. Equations [A-2] can be rewritten in the

following form:

$$\sum_i (A^k_{qi} - \delta_{iq}\delta_{kj})S^j_i = 0 \qquad j,k = 1,2,\ldots,n. \qquad \text{[A-3]}$$

The last set consists of n^2 linear equations for the n^2 unknowns S^j_i. By taking first j = constant we can solve the n equations for the unknowns S^j_k $(k = 1,2,\ldots,n)$ and then proceed to the following superscript. The corresponding values of the vectors $\mathbf{R}^k$ are obtained now from [14]. Once all the vectors **R** and **S** are known, the matrix **w** can be obtained from [15]:

$$w_{ij} = \sum_k \lambda_k S^k_i R^k_j. \qquad \text{[A-4]}$$

The flow rates can now be obtained as follows: all the modified flow rates $w_{ij}(i \neq j)$ are given by the off-diagonal elements of **w**. The actual flow rates W_{ij}, the outflow rates W^e_j and inflow rates W^f_i can be calculated by [1]–[4], provided the volumes are known.

The same results can also be obtained by injection of the tracer into each of the vessels and measuring the resulting concentration history in one of them or by some other experiments of n separate measurements. Thus, it follows that n tracer measurements (concentration curves) are sufficient, in principle, for the identification of all the parameters needed for a compartmental model consisting of n vessels.

APPENDIX B

We develop here the expression [19] for the probability P_{ij} of a particle at vessel i to pass (at least once) at vessel j.

Consider an (imaginary) experiment in which tracer is introduced as a pulse at $t = 0$ in vessel m. Without loss of generality, we seek the probability P_{mn}, where n is also the number of vessels. Assume that every tracer particle is tagged and counted (imaginarily) when it first enters n. The probability P_{mn} is then the ratio of the total number of these particles to the total number of particles introduced into vessel m. The fraction of particles at vessel i at time t is the transition probability $p_{mi}(t)$. Denote by $x_{mi}(t)$ the fraction of tagged particles at the same site and time. The equations and initial conditions for $x_{mi}(t)$ are similar to those for the transition probabilities (section 2):

$$\frac{dx_{mi}}{dt} = \sum_{k=1}^{n} x_{mk}w_{ki} \qquad i = 1,2,\ldots,n-1, \qquad \text{[B-1]}$$

$$x_{mn}(t) = p_{mn}(t), \qquad \text{[B-2]}$$

$$x_{mi}(0) = 0 \qquad i = 1,2,\ldots,n. \qquad \text{[B-3]}$$

Using [B-2], [B-1] can be rewritten in the form:

$$\frac{dx_{mi}}{dt} = \sum_{k=1}^{n-1} x_{mk}w_{ki} + p_{mn}w_{ni}. \qquad \text{[B-4]}$$

Denote now the fraction of untagged particles at vessel i at time t by $\theta_{mi}(t)$:

$$\theta_{mi} = p_{mi} - x_{mi} \qquad i = 1,2,\ldots,n. \qquad \text{[B-5]}$$

The equations and initial conditions for θ_{mi} are then derived from [B-1]–[B-4], [8] and [10]:

$$\frac{d\theta_{mi}}{dt} = \sum_{k=1}^{n-1} \theta_{mk}w_{ki} \qquad i = 1,2,\ldots,n-1. \qquad \text{[B-6]}$$

$$\theta_{mi}(0) = \delta_{mi}. \qquad \text{[B-7]}$$

The solution for the last set of equations can be found in the same way as the solution for the transition probabilities (see section 2). The eigenvalues are obviously different because here the generator matrix is of the order $n-1$ and not n as was the case in section 2.

The probability P_{mn} is given by the following:

$$P_{mn} = \sum_{k=1}^{n-1} w_{kn} \int_0^\infty \theta_{mk}(t)\,\mathrm{d}t. \qquad \text{[B-8]}$$

Introducing [B-5] into [B-8] the following is obtained:

$$P_{mn} = \sum_{k=1}^{n} w_{kn} \int_0^\infty (p_{mk} - x_{mk})\,\mathrm{d}t = \sum_{k=1}^{n} w_{kn} \int_0^\infty p_{mk}\,\mathrm{d}t - w_{nn} \int_0^\infty p_{mn}\,\mathrm{d}t - \sum_{k=1}^{n-1} w_{kn} \int_0^\infty x_{mk}\,\mathrm{d}t$$

$$= -w_{nn} \int_0^\infty p_{mn}\,\mathrm{d}t - \sum_{k=1}^{n-1} w_{kn} \int_0^\infty x_{mk}\,\mathrm{d}t \qquad \text{[B-9]}$$

where the last relation was obtained from [B-8], bearing in mind that $m \neq n$. Observing now [B-4] it can be seen that the following relationship holds:

$$\int_0^\infty x_{mk}\,\mathrm{d}t = K'_k \int_0^\infty p_{mn}\,\mathrm{d}t. \qquad \text{[B-10]}$$

Thus [B-9] yields the following for the probability P_{mn}:

$$P_{mn} = K_n \int_0^\infty p_{mn}\,\mathrm{d}t$$

$$K_n = -\left(w_{nn} + \sum_{k=1}^{n-1} w_{kn} K'_k\right) \qquad \text{[B-11]}$$

where K_n (as also K'_k) is a constant depending on the parameters W_{ij} and most important, does not depend on m. Since m and n are arbitrary indices, [A-11] holds for every pair of indices i, j:

$$P_{ij} = K_j \int_0^\infty p_{ij}(t)\,\mathrm{d}t. \qquad \text{[B-12]}$$

K_j can be evaluated from the following identity:

$$P_{jj} = K_j \int_0^\infty p_{jj}(t)\,\mathrm{d}t = 1. \qquad \text{[B-13]}$$

Thus

$$P_{ij} = \frac{\int_0^\infty p_{ij}(t)\,\mathrm{d}t}{\int_0^\infty p_{jj}(t)\,\mathrm{d}t}. \qquad \text{[B-14]}$$